JOURNAL OF MATERIALS SCIENCE **36** (2001) 1219–1225

Elastic constants of porous silver compacts after acid assisted consolidation at room temperature

O. YEHESKEL
Department of Materials Engineering, Ben-Gurion University of the Negev, Beer Sheva 84105, Israel; Nuclear Research Center Negev, P.O. Box 9001, Beer-Sheva 84190, Israel

M. SHOKHAT
Nuclear Research Center Negev, P.O. Box 9001, Beer-Sheva 84190, Israel

M. RATZKER, M. P. DARIEL
Department of Materials Engineering, Ben-Gurion University of the Negev, Beer Sheva 84105, Israel
E-mail: yeheskelori@hotmail.com

Acid assisted consolidation (AAC) is a technique that provides elevated levels of cohesiveness to silver powder compacts without recourse to a high temperature treatment. Ultrasonic techniques were used to measure the elastic constants of high purity silver compacts as a function of several processing variables. The elastic moduli of untreated (NT) samples were found to be significantly lower than those of samples that had undergone AAC and compacted at the same pressure. Post compaction sintering increases the elastic constants of both AAC and NT samples. The results indicate that the elastic constants are dependent not only on the density that was attained but also on the processing route that was followed. The elastic constant of a porous metal, M, can be expressed as $M = M_0 g\varphi$, where M_0 is the elastic modulus of the bulk metal, g is a geometrical factor that reflects the interparticle contact area and φ is a quality factor that depends on the nature of the interparticle interfaces. The results suggest that sound wave velocity is a parameter more appropriate than density for predicting the elastic moduli of porous metallic compacts.

1. Introduction

According to the conventional powder metallurgy approach, cohesive solids are produced from starting powders by the combined effect of pressure and temperature, applied either sequentially or simultaneously. Sintering of the powder particles takes place in the course of the high temperature treatment. The properties of the final product, i.e. elastic moduli, strength, conductivity and resistance to wear, depend on the density attained during sintering. Recently, an alternative technique has been put forward for consolidating silver powder. This technique, denoted acid assisted consolidation (AAC), was developed in order to transform a loose powder into a cohesive solid by applying low pressure and no exposure to elevated temperature. The technique consists of consolidating under low pressure silver powder that had previously been treated in a dilute fluoroboric acid (HBF_4) solution for a short period of time. The technique was developed as a method of consolidation a mercury-free filling material for dental restorative use [1–4]. The results have shown that the strength of the acid-compacted products depends strongly on the pressure applied during compaction and reaches values comparable to those of bulk silver for compacting pressures lower than 1 GPa.

The fluoroboric acid acts as a fluxing agent, removes the surface oxide layers and induces a cold-welding-like effect between the silver particles. The pressure applied during compaction determines the density and the strength of the silver compact. Preliminary studies have shown that the compaction pressure also determines the elastic moduli of the silver compacts [4]. In fact the elastic moduli closely reflect the density and indirectly the pressure exerted during compaction.

Numerous studies have been carried out over the past years in order to derive the relations that prevail between the relative density, or porosity, and the elastic moduli of sintered metallic and ceramic materials [5–12]. In these studies porous samples were prepared by sintering compacted metallic or ceramic powders to controlled levels of density and determining their elastic moduli, most often by means of sound wave velocity measurements. The results of these studies were used to determine the relationship between elastic moduli and porosity. Numerous expressions that describe the elastic modulus–porosity relations [6, 9–12] can be found in the literature. The analysis of the ultrasonic data obtained from powder compacts that had been sintered to different levels of density is a highly complex problem, affected by numerous parameters that continuously change in the

course of a sintering cycle [12]. As the sintering process proceeds, both the nature and the extension of the contact area between adjacent particles undergo changes.

The relative density range, attained in the course of conventional sintering of metals, extends usually from 0.7 to almost full density. By using the AAC technique, this effect can be followed over a relative density range that extends from 0.5 to almost full density. Moreover, the density is increased only by the room temperature plastic deformation caused by the compacting pressure and not by any sinter-diffusion processes as in sintering. Thus, one can assume that the nature of the inter-particle contact area is not affected by any mass transport effect, only its extension changes. The comparison of the measured elastic moduli of samples prepared by both above-mentioned methods should allow evaluating the relative contribution of the extension and of the nature of the inter-particle contact area on the elastic constants of porous samples.

2. Experimental procedure

2.1. Powder characterization

Pure (99.9 wt%) silver powder from two sources was used in the present study. The details regarding the particle size, particle shape, surface area determined by the Brauner Emmett Teller (B.E.T) method, apparent density (AD), tap density (TD), and the suppliers are shown in Table I. The particle shape was determined by scanning electron microscopy (SEM), Fig. 1.

2.2. Sample preparation

The acid-treatment consisted of immersing the silver powder in dilute fluoroboric acid and stirring for 5 min at 500 rpm. Powder aliquots, weighing 0.6–$1.5 * 10^{-3}$ kg, were stirred in 200 ml dilute (3.5 vol. %.), fluoroboric acid. The powder settled and the slurry was placed in an Inconel 718 mold designed for producing near-net-shape samples. The slurry was uniaxially compressed in the pressure range of 50–900 MPa. Compaction pressure values were accurate within 10 MPa and compaction dwell time was 2 min. In the course of the compaction, the residual dilute acid was squeezed out the mold and absorbed by paper tissue. For the density and elastic moduli measurements, 8 mm diameter by 1.5–3 mm thick discs were prepared with plane parallel faces. Both AAC and untreated (NT) samples were prepared from powder A′. The compaction pressure of the AAC samples from powders B′ and C′, was about 300 MPa. For all the powders, 3–5 samples

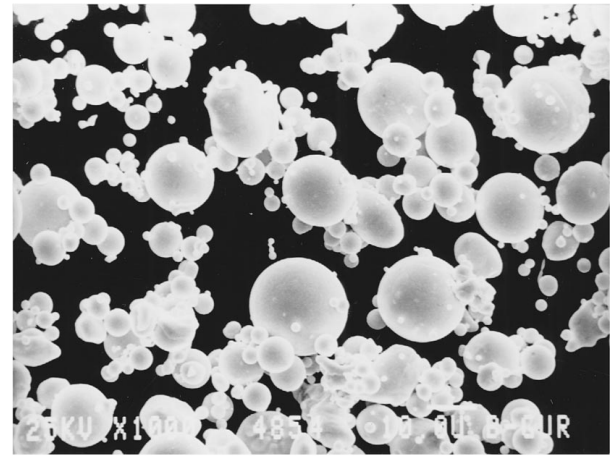

(a)

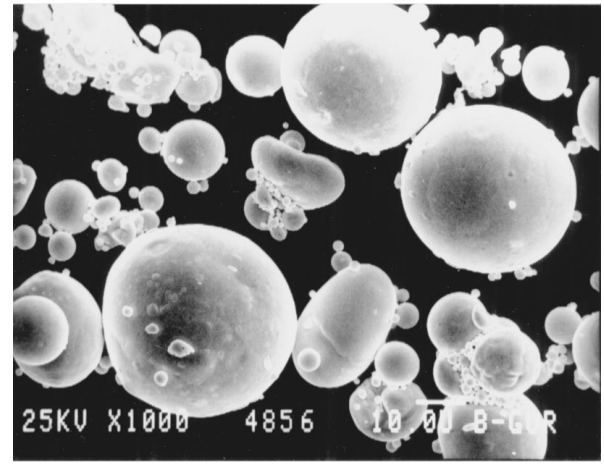

(b)

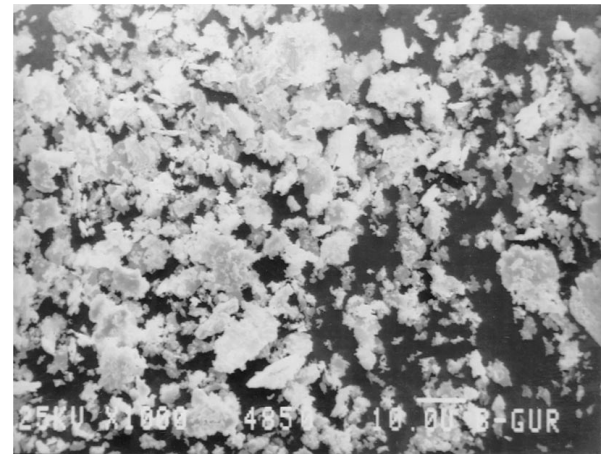

(c)

Figure 1 SEM images of the atomized (HJE) spherical silver particles (a) powder A, (b) powder B and of the irregular particles (c) powder C.

TABLE I Characteristics of the powders that were used: particle size, particle shape, surface area as determined by B.E.T., apparent density (AD), tap density (TD), and vendor's name

Powder notation	Particle size [mesh]	Particle size [μm]	Particle shape	B.E.T. [m^2kg^{-1}]	AD [%]	TD [%]	vendor
A′	−500	−20	spherical	0.212	0.382	0.553	HJE*
B′	−325/+500	−44 + 20	spherical	0.180	0.486	0.627	HJE
C′		−1	dendritic	1.15	0.220	0.303	CA**

*HJE- HJE Company. Glen Falls, NY. **CA-Consolidated Astronautics.

were compacted at each compaction pressure. The acid-treated samples were kept under vacuum (3 Pa) in a desiccator for periods extending from 3 to 30 days.

A few A′-type powder samples underwent, prior to the AAC, a heat treatment under vacuum (0.2 Pa) at 350°C for 18 hours (HT-A′ samples). The purpose of the heat treatment was to study the effect of a stress relief on the density and the elastic moduli. Some NT-A′ and A′ samples underwent sintering at 0.8 T_m (714°C, T_m, melting point of silver) for one hour. Prior to sintering, the samples were heated to 250°C under vacuum in order to remove the residual moisture. These A′ samples were compacted in the 50–500 MPa range and the NT-A′ samples in the 300–500 MPa range.

2.3. Sample characterization

The characterization of the samples included density and sound wave velocity, (SWV), measurements and, for selected samples, fractography by scanning electron microscopy (SEM). The density, ρ, was measured by the liquid displacement (Archimedes) method in distilled water the density of which was corrected for temperature variations. The accuracy of the density determination is estimated to be better than ±0.3%.

Sound wave velocity measurements were performed along the compacting direction by the pulse-echo method according to which the time of flight (*tof*) of short duration ultrasonic pulses is measured. The (*tof*) is the time for a stress wave (acoustic wave) to travel back and forth along the length of the sample, L. Details of the measurements were given elsewhere [12]. Each sample was ground to plane-parallel faces better than $\pm 3 \times 10^{-6}$ m. The accuracy of the sample height measurement was $\pm 2 \times 10^{-6}$ m. The frequency of the pulse generating transducers, both for longitudinal and transverse waves, was 5 MHz. The sound wave velocity, V_i, was calculated according to:

$$V_i = \frac{2L}{(tof)_i} \tag{5}$$

where the index i indicates the longitudinal or the transverse mode (denoted l and t, respectively). The longitudinal velocity was measured by coupling the transducer to a wave-guide using a thin oil film. To prevent sample contamination, a thin rubber layer or aluminum or a foil was inserted between the wave-guide and the porous sample. At least three *tof* measurements were made averaging 100–1000 waveforms. Difficulties were encountered in trying to measure sound velocity in NT-A′ samples. Most of these samples broke up under the pressure at which the transducer was pressed and some disintegrated during grinding. The accuracy of the sound wave velocities was about ±0.3% for the AAC and about ±4% for the NT-A′ samples. The large uncertainty in the NT-A′ samples is due the presence of cracks/microcracks. For samples that underwent an insufficient acid treatment, e.g. powder C′, the variation of the sound wave velocity was of the order of ±2%.

2.4. Elastic moduli measurements

The shear modulus, G, and Young's modulus, E, are calculated according to Equations 6 and 7 respectively [13, 14]. The Poisson's ratio, ν is calculated according to Equation 8 and the bulk modulus is derived from the measured G and E values according to the elasticity theory [15].

$$\text{Shear modulus} \qquad G = \rho V_t^2 \tag{6}$$

$$\text{Young's modulus} \quad E = \rho V_l^2 (1+\nu)(1-2\nu)/(1-\nu) \tag{7}$$

$$\text{Poisson's ratio} \qquad \nu = \frac{E}{2G} - 1 \tag{8}$$

Usually the elastic constants in porous materials are plotted against the porosity, see section 3.3. Porosity, p, is the volume fraction of pores and is defined by $p = 1 - \rho/D_T$, where D_T is the theoretical density of the material. In the present study D_T for pure silver was taken as 10,505 kgm^{-3}, which is an average of the various values reported for pure silver in the literature [14, 16–18].

3. Results and discussion

3.1. The effect of the compaction pressure on the density of A′ and NT-A′ silver compacts

The density of the various acid-treated powders (A′, B′, and C′), the untreated and heat-treated (NT-A′ and HT-A′, respectively), as a function of the compaction pressure is shown in Fig. 2. The behavior shown in Fig. 2 is consistent with the qualitative description of metal powder compaction given by German [19]. The density of the NT-A′ samples compacted in the 0–300 MPa pressure range was slightly higher than that of the AC samples. This can be attributed to the effect of the fine oxide film on the original NT-A′ particles that reduces the inter-particle friction, whereas, the acid-treatment removes the oxide film and promotes adherence between adjacent particles as apparent in Fig. 3a. Adherence increases the coefficient of friction resulting in a slightly lower density at low compacting pressure in

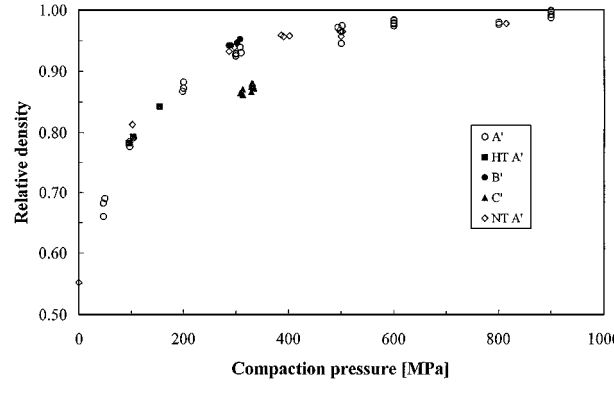

Figure 2 The dependence of the density of compacted samples of powder A′ on the compaction pressure. The density of powders B′ and C′ after compaction at about 300 MPa is shown for comparison.

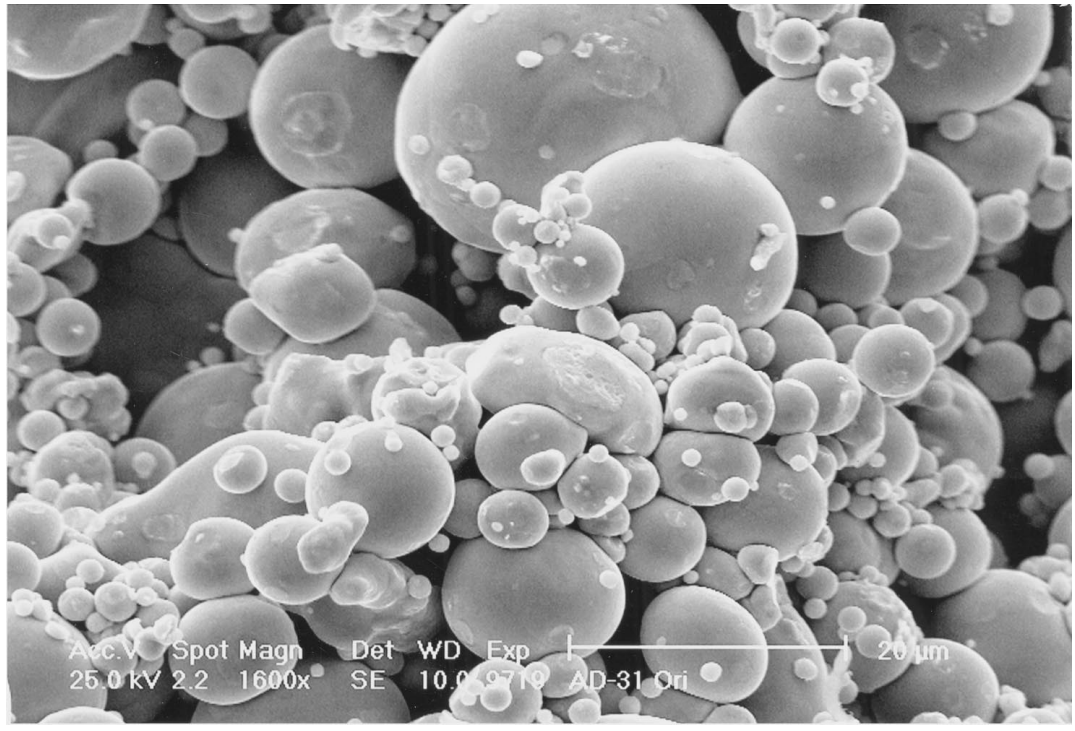

(a)

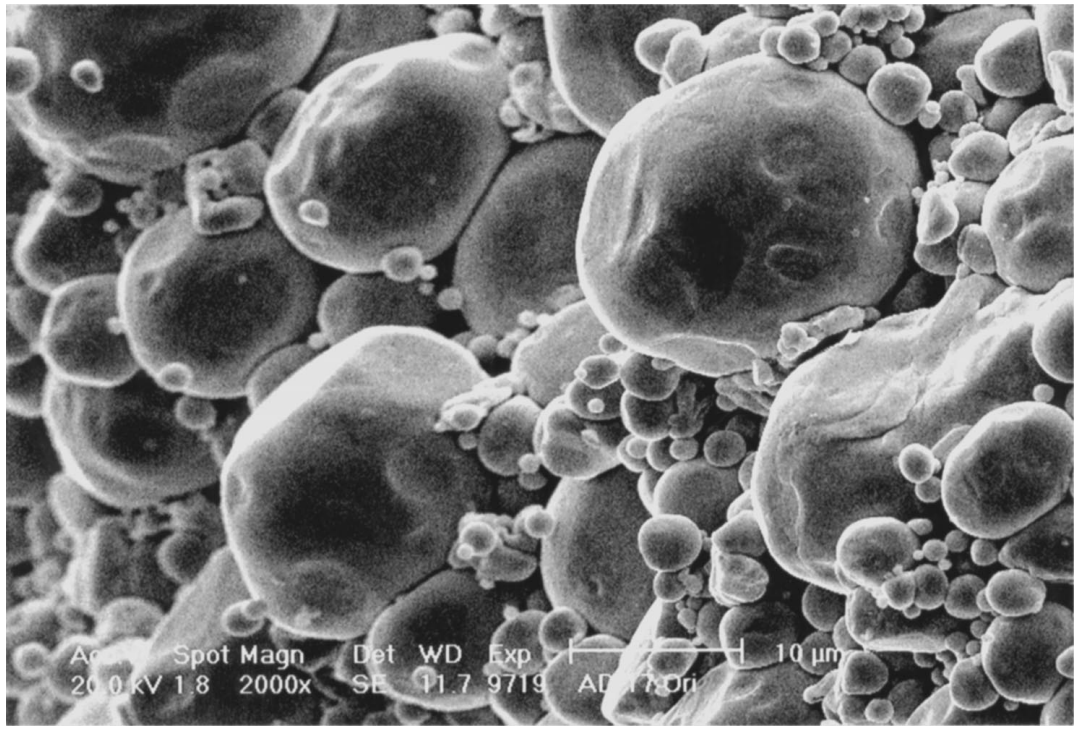

(b)

Figure 3 (a) The beginning of localized deformation in an A′ sample that was compacted at 50 MP; (b) Localized contact area in NT-A′ sample that was compacted at 200 MPa, notice the crack besides the large particle.

the A′ samples. In the high-pressure range, both NT-A′ and A′ samples attain the same level of density. In this pressure range, the oxide film on the NT-A′ samples has broken down and some inter-particle adherence takes place.

Two other features in Fig. 2 are noteworthy:

a) The density of C′ samples is significantly lower than that of A′ and B′ samples. This difference is probably due to the different particle shape of the C′ particles.

b) The heat-treatment did not affect the density of the AAC samples.

3.2. The effect of compaction pressure on the sound velocity and elastic constants of acid-treated silver powder compacts

The dependence of the longitudinal and shear velocities on the compaction pressure of powder A′ and HT-A′ is shown in Fig. 4. The sound velocity of the

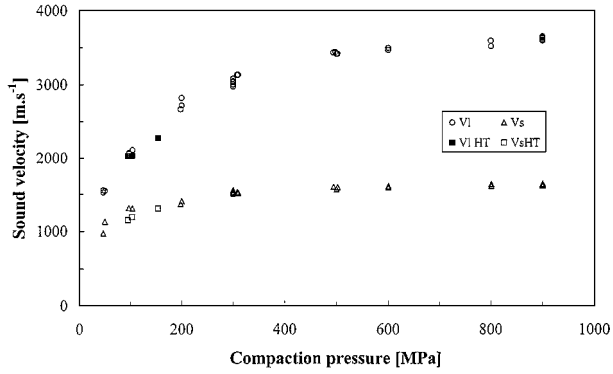

Figure 4 The dependence of the longitudinal (Vl) and shear (Vs) sound wave velocities of A′ samples on the compacting pressure. Note the slightly lower values for the heat-treated samples (HT).

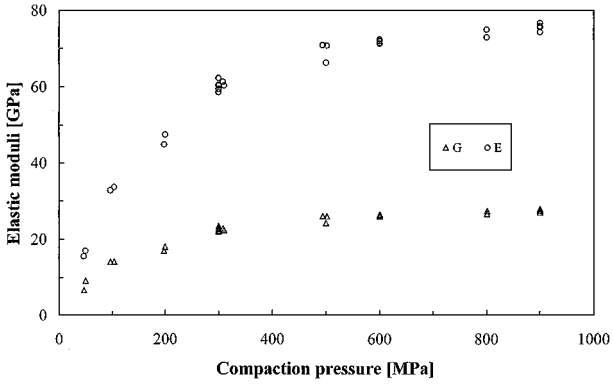

Figure 5 The dependence of the Young's (E) and shear (G) moduli of A′ samples on the compacting pressure.

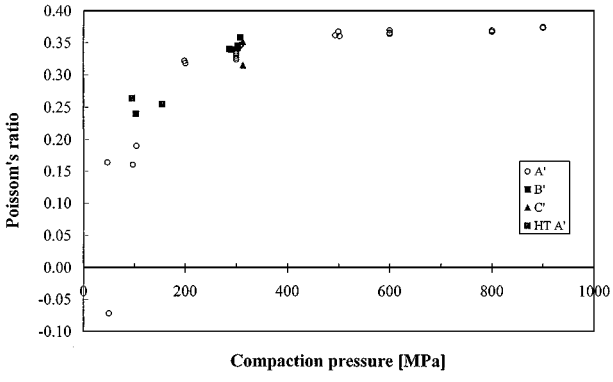

Figure 6 The variation of Poisson's ratio with the compaction pressure of AAC silver compacts.

heat-treated samples is slightly lower than those of the regular AAC samples. The elastic constants of AAC silver powders increase with the compaction pressure as shown in Fig. 5 for G and E and in Fig. 6 for the Poisson's ratio.

3.3. The effect of porosity on the elastic properties of NT-A′ and A′ silver powder compacts

The dependence of the measured Young's and the shear moduli of the A′ samples on the porosity were fitted to two commonly used expressions and shown in Fig. 7.

$$M = M_0(1 - ap) \tag{9}$$

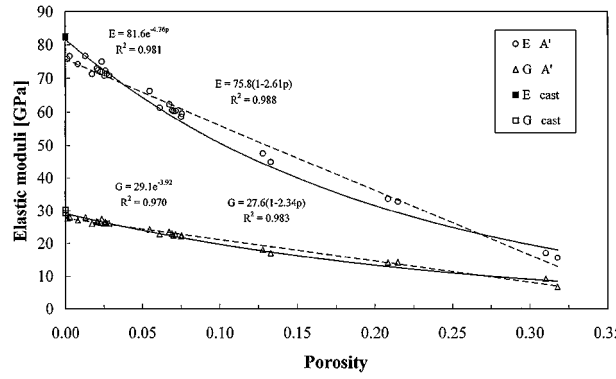

Figure 7 The elastic moduli against the porosity of A′ silver compacts. The solid and the dashed lines designate the estimated elastic moduli from exponential and linear expressions respectively.

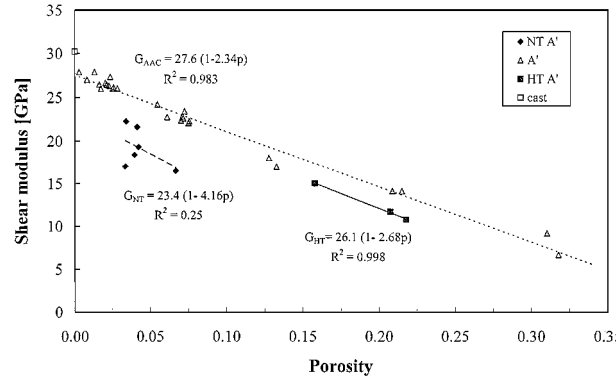

Figure 8 Effect of porosity and of the processing route, on the shear modulus of silver compacts. (The dotted, solid and broken lines designate the linear regression correlation for the A′, HT-A′, and NT-A′ samples respectively).

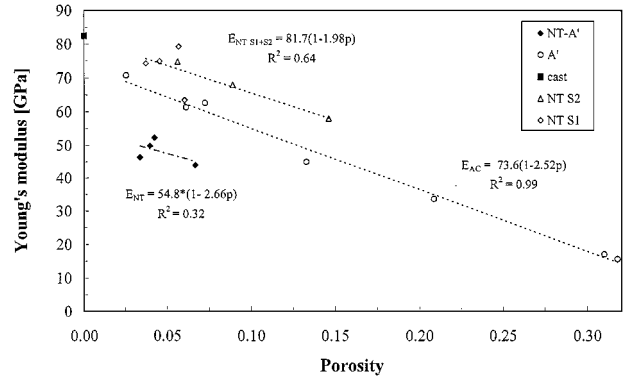

Figure 9 The Young's modulus of the various silver compacts of powder A′, grouped according to their processing, as a function of the porosity.

$$M = M_0 \exp(-bp) \tag{10}$$

where M is the elastic moduli of the porous sample, M_0 is the elastic modulus of the solid bulk, and a and b are constants. Since there is no significant difference between the two fits, the linear dependence will hereafter be used.

The scatter of the results for the NT-A′ samples probably reflects the presence of multiple cracks. The presence of multiple cracks and the low interparticle bond strength can be deduced from Fig. 3b. The 'elastic moduli' of these samples are reported only in order to provide a reference frame for the effect of the AC and sintering treatments (Figs 8 and 9). Relatively reliable

sound wave velocity measurements were carried out on NT-A′ samples that had been compacted in the intermediate pressure range of 300–500 MPa. In the NT-A′ samples the attenuation of the longitudinal waves was very high and only in two samples could the transverse velocity be measured. Equation 7 was used to calculate the Young's modulus and assuming that the Poisson's ratio of the NT-A′ samples was the same as that of A′ samples at similar density (porosity). The values of the Poisson's ratio were derived by interpolation from Figs 6 and 2. For two NT-A′ samples, compacted at 500 MPa, the interpolated value compares well with the measured value. It clearly shown that the values of the 'elastic moduli' of the NT-A′ samples are approximately 25% lower than the elastic moduli of the acid-treated samples. The lower values are attributed to the presence of the surface oxide layer that impedes particle bonding but breaks probably down above 300 MPa and allows partial bonding between the NT-A′ particles to take place. The elastic constants of samples at the same density rank $G_{A'} > G_{HT\text{-}A'} > G_{NT\text{-}A'}$, as shown, for example in Fig. 8. These results clearly show that the elastic moduli depend not only on density (porosity) but also on the processing route that was followed.

3.4. The effect of the particle size and shape on the elastic moduli

The elastic moduli (M) and the density depend on the initial particle shape and can be ranked as $M_B' > M_A' > M_C'$. In order to check whether the dependence of the elastic moduli arises only through the dependence of the density or possibly to some additional causes, the measured values of samples of equal density have to be examined. The results show that the elastic moduli of A′ and B′ samples fall within a 5% range, whereas, the difference between A′ and C′ samples is about 25%. These differences can be attributed to the difference in shape and surface area of the particles, see Table I.

3.5. Effect of the sintering treatment on the elastic properties of A′ and NT-A′ silver compacts

In order to gain further insight into the effect of sample processing route on the elastic moduli of silver, powder sintering treatments were carried on both A′ and NT-A′ silver compacts. The sintering treatment increases the elastic moduli of the A′ samples by about 20%, and those of the NT-A′ samples by 60%. Samples, after acid treatment, compacted at elevated pressure, swelled after a sintering treatment due to the expansion of the residual liquid in closed pores. No swelling was observed in samples compacted below 300 MPa. Swelling, due to residual humidity, was also observed in NT samples that had been compacted above 400 MPa. Sound velocity in these samples (denoted NT S1) was measured before and after the sintering treatment. A second set of NT samples (NT S2) were compacted at low pressure to avoid retention of humidity and the sound velocity measured only after the sintering treatment. The dependence of the Young's modulus on porosity for samples that had undergone the three different processing routes is shown in Fig. 9. It shows that for all porosity values, the Young's moduli rank $E_S > E_{AAC} > E_{NT}$. These results clearly show that density is not the sole parameter that determines the elastic properties of metallic compacts and that additional factors should be considered. In particular, we believe that the interparticle contact area and the quality of the bond established across the inter-particle contact area determine the elastic moduli. Thus, the elastic moduli, M, of partially densified materials can be expressed as:

$$M = M_0 g \varphi \tag{11}$$

where M_0 is the modulus of defect free material, g is a geometrical factor that gives measure of the contact area between the particles, and φ is a factor that reflects the quality of interparticle bond. The geometrical factor depends on the interparticle contact area attained either after plastic deformation or as the outcome of a sintering treatment, $g = 0$ at tap density and $g = 1$ at full density. The quality factor, $\varphi = 0$, for a loosely packed untreated powder and $\varphi = 1$ for a material in which the bond across the particle interface is of same quality as within a defect free material. The dependence of g on the density can be derived from existing models [20, 21]. The extrapolated values of $E_{g=1}$ the Young's modulus, for the various processing routes, assuming a linear dependence on density (Equation 9), are given in Table II. The extrapolated $E_{g=1}$ can be used to determine the values of φ that are clearly process dependent.

TABLE II The Young's modulus at full density, $E_{g=1}$ and the quality factor, φ of the four processing routes: sintering, S, acid assisted consolidation, AAC, heat treatment followed by AAC, HT and untreated, NT

Processing route → Property ↓	S	AAC	HT	NT
$E_{g=1}$	82	75	65	55
φ	1.0	0.92	0.79	0.67

E in [GPa] and φ is a dimensionless factor.

3.6. Sound wave velocity as a predictor to the sintered state

The results that were obtained above clearly indicate that the commonly used criterion for the elastic constants of sintered materials, namely the density, does not provide an unambiguous description of the sintered state. The elastic moduli, as shown in Fig. 9, are process dependent and so is the sound wave velocity. Processing routes affect the sound wave velocity either by change in the acoustic path-length and/or change in the quality of the interparticle contact area. According to Equation 11 the geometrical factor reflects the change in the acoustic path-length and the quality factor stands for the quality of the interparticle contact area. The plot of the normalized Young's modulus, $E^* = E/E_0$, vs. the normalized sound wave velocity $V_L^* = V_L/V_{L0}$ yields a single curve as shown in Fig. 10.

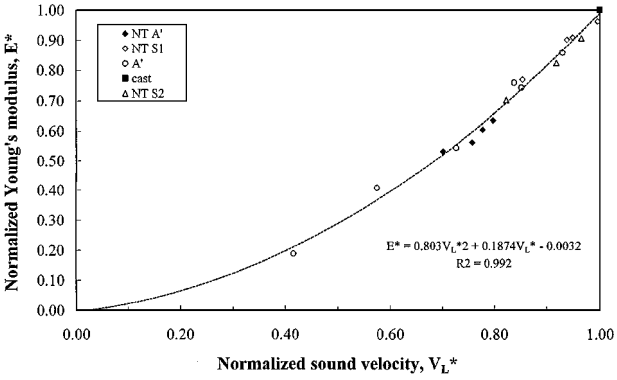

Figure 10 The normalized Young's modulus of porous samples as a function of the normalized longitudinal velocity. (Data points from Fig. 9).

A one-to-one correspondence prevails between the sound velocity and the elastic moduli, whatever the processing route followed. These results suggest that sound wave velocity may be a more appropriate parameter than commonly used density for describing the sintered state, i.e. the elastic moduli, of powder compacts [12].

4. Conclusions

The following conclusions can be drawn from the present study:

1. The dependence of the density of acid assisted consolidated and of untreated silver powder compacts on the compacting pressure is similar to that described by German [19] .

2. Acid-assisted consolidation, even though involves no elevated temperature treatment, is a highly effective process that yields elastic moduli that are only slightly inferior to those of bulk silver.

3. The elastic moduli-porosity relationships follow linear dependence in the 0.35–0 porosity range.

4. Compacts of silver powder that did not undergo acid treatment contain cracks and their elastic properties are by about 25% lower than those of AAC samples.

5. Sintering at elevated temperature increases the elastic properties. Its effect on AAC silver compacts is moderate in contrast to its effect of plain cold-compacted silver. In the latter case, stiffness is almost exclusively due to the bonding established during the sintering treatment.

6. The elastic moduli of silver compacts are an easily measurable physical quantity that characterizes the state of the partly dense compacts and are ranked as follows: $M_S > M_{AAC} > M_{NT}$.

7. We suggest to describe the elastic moduli of porous metals by $M = M_0 g\varphi$, where M_0 is the elastic moduli of defect free material, g is a geometrical factor and φ is a quality factor.

8. Sound wave velocity is a predictor more appropriate than density in describing the elastic moduli of metallic compacts.

Acknowledgements

The authors express their gratitude to Mr. J. Eliashevich for his assistance in the heat treatment. To Mrs. M. Pinkas and Dr. U. Admon for SEM micrographs and to Dr. J. Koresh for B.E.T. measurements and to Mr. O. Tevet for his valuable help in carefully checking the ultrasonic results.

References

1. M. P. DARIEL, D. S. LASHMORE and M. RATZKER, *Dental Mater.* **11** (1995) 208.
2. M. P. DARIEL, U. ADMON, D. S. LASHMORE, M. RATZKER, A. GIUSEPPETTI and F. C. EICHMILLER, *J. Mater. Res.* **19**(3) (1995) 505.
3. M. P. DARIEL, M. RATZKER, D. S. LASHMORE and P. BENNETT, in Proceedings of the Second Pacific Rim International Conference on Advanced Materials and Processing, edited by K. S. Shin, J. K. Yoon and S. J. Kim (The Korean Institute of Metals and Materials, Korea, June 1995) p. 377.
4. M. P. DARIEL, M. RATZKER and F. C. EICHMILLER, *J. Mater Sci.* **34** (1999) 2601.
5. F. P. KNUDSEN, *J. Am. Ceram. Soc.* **42** (1959) 376.
6. J. C. WANG, *J. Mater. Sci.* **19** (1984) 801.
7. *Idem., ibid.* **19** (1984) 809.
8. J. P. PANAKKAL, H. WILLEMS and W. ARNOLD, *J. Mater. Sci.* **25** (1990) 1397.
9. E. A. DEAN and J. A. LOPEZ, *J. Am. Ceram. Soc.* **66**(5) (1985) 366.
10. K. K. PHANI and S. K. NIYOGI, *ibid.* **70**(12) (1987) C-362.
11. J. R. MOON, *Powder Metall.* **32**(1) (1989) 47.
12. O. YEHESKEL and O. TEVET, *J. Am. Ceram. Soc.* **82**(1) (1999) 136.
13. Standard practice for measuring ultrasonic velocity in materials, ASTM designation E 494-95, March 1995.
14. H. M. LEDBETTER, N. V. FREDERICK and M. W. AUSTIN, *J. Appl. Phys.* **51**(1) (1980) 305.
15. S. P. TIMOSHENKO and J. N. GOODIER, "Theory of Elasticity," International student ed. (McGraw-Hill, New York) (1970) p. 485.
16. JCPDS, Powder Diffraction File, X-ray Card # 4-0783.
17. O. L. ANDERSON, in "Physical Acoustics," Vol. III, Part B, edited by W. P. Mason (Academic Press, New York, 1965) p. 43.
18. H. LEDBETTER, in "Dynamic Elastic Modulus Measurements in Materials," edited by A. Wolfeneden (STP 1045, ASTM, 1990) p. 143.
19. R. M. GERMAN, "Powder Metallurgy Science," 2nd ed. (MPIF, Princeton, USA, 1994) p. 205.
20. H. F. FISCHMEISTER, E. ARZT and R. L. OLSON, *Powder Metall.* **4** (1978) 179.
21. E. ARZT, *Acta Metall.* **30** (1982) 1883.

Received 24 February
and accepted 30 August 2000